# *A Topology Morphing Multi-Element Resonant Converter with Wide Voltage Gain Range*

Liang Yang, Yifeng Wang, Chengshan Wang, Wei Li, Mengying Chen
School of Electrical and Information Engineering
Tianjin University
Tianjin, China
zyangliang@tju.edu.cn

***Abstract*—A topology morphing multi-element resonant converter (MRC) is proposed in this paper. The converter introduces two auxiliary switches and is able to exchange its equivalent topology flexibly. Consequently, widely adjustable voltage gain from 0 to 8 is acquired within a small operating frequency range, which contributes to highly efficient conversion as well. The resonant parameters of the converter are also designed and tested by a prototype. The experimental results demonstrate that the converter harvests relatively high efficiencies among the entire input voltage variations from 25V to 300V, and the highest efficiency point has reached 98.1%.**

***Keywords—Topology morphing; multi-element resonant converter; high efficiency; LCLCL converter; CLTCL converter***

## I. INTRODUCTION

The resonant converters are famous for many fruitful benefits including high efficiency conversion, high frequency operation, low EMI, and therefore have been extensively applied.

Simply classified by the relation between the input and the output voltages, resonant converters can be divided into the step-up type and the step-down type. Presently, large numbers of researches have been conducted on the latter type, since the step-down converters are more likely suitable for comprehensive applications. Usually, they are always used as the renewable energy production, the electric vehicle charger, the Li battery charger, the LED driver, the switched mode power supply [1-5].

However, for applications like photovoltaic generation and grid-connected wind power generation, the step-up resonant converters are preferred. Despite some step-down converters, discussed in literatures [6-9], can operate at the step-up state also, their voltage gains barely meet the application demands since relatively high step-up characteristic is required.

Several high step-up resonant converters have been reported in previously published works [10-14]. Papers [10-11] are devoted to realize highly efficient conversion on the basis of the LLC converter through proper parameter selection, and every possible operating mode of the LLC converter are studied and compared in detail. Then a novel parameter design method of peak gain placement is discussed and ensures the converter high efficiency. Whereas, owing to the inherent contradiction between the efficiency and voltage gain range of the LLC topology, the input voltage range (25-38V) of this converter is not wide enough for the high step-up applications, whose inputs are always fluctuating violently. In [12], a dual-transformer structure LLC converter is described. The converter operates as the normal LLC converter around the rating working point. While in the case of insufficient power and low input voltage, the auxiliary transformer (AT) is conducted. The output voltage of the AT is superimposed onto that of the conventional LLC part, and thus high voltage gain is ensured even at the light load. However, this circuit still suffers from the same problem as the narrow input voltage range. Then the idea is further expanded in reference [13], where the dual-transformer topology is also applied. This converter achieves wide voltage gain range from 2.1 to 8.4 for a constant output voltage of 210V by means of changing the equivalent magnetizing inductor. Under the circumstance where low input voltage is provided, it works as the traditional LLC converter with a small magnetizing inductor for high voltage gain; while for higher input voltage case, the AT is enabled to increase the equivalent magnetizing inductor, and thus the conduction loss is restrained. This converter can be switched within very narrow frequency range, which also avoids the high frequency losses. Nevertheless, it still faces challenges as incapability of step-down operation and extra introduced diode rectifier bridge. Moreover, the auxiliary switches adopted to control the AT are arranged in the primary low-voltage side, in which the primary current is much larger than that of the secondary side, and relatively larger primary conduction losses are inescapable as the following outcomes. Related to the above comments, an outstanding resonant converter for the high step-up application must possess characteristics of broader voltage ranges as well as high efficiency.

This paper proposes a topology morphing MRC. By properly tuning the controlling signals, the auxiliary switches enable and disenable the AT, and thus the equivalent topology can change over between the LCLCL type [15] and the CLTCL type [16]. This morphing ensures the MRC very large voltage gain range and can both work under step-up and step-

down conditions. The operating frequency is also confined within a narrow range near the rating point, which guarantees high efficiency as well. A 200W prototype is fabricated to verify the theoretical analyses. The output voltage is regulated constantly at 200V with input voltage from 25V to 300V, and the peak efficiency is measured as high as 98.1%.

## II. Topology Evolution

The LCLCL and CLTCL converters are two types of MRCs, both of which own multiple resonant points and thus present beneficial traits comparing with the traditional LLC-based topologies.

In Fig. 1, the circuit diagram of LCLCL and the corresponding DC voltage gain curves under different loads are shown. The resonant tank of this circuit is composed of a high frequency transformer, one pairs of series- and parallel-connected LC components respectively. The parallel LC forms a notch architecture and thereby introduces a unique resonant zero point (RZP) into the gain curves, at which the voltage gain is fixed at zero regardless of the load variations. The RZP not only ensures a wide adjustable voltage gain range starting from zero, but also provides inherent over-current protection even for the short-circuit case. Besides, by appropriate design of the resonant parameters, this converter can transfer 1st and 3rd harmonics simultaneously, which contributes to a restricted circulating power [15].

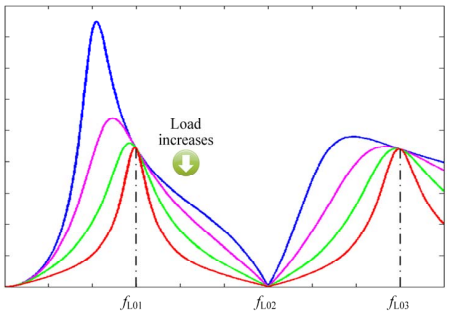


Fig. 1. DC voltage gain curves of the LCLCL topology.

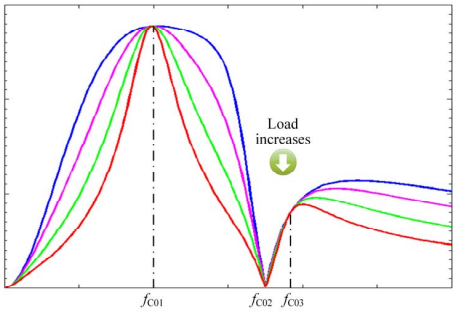


(b)

Fig. 2. DC voltage gain curves of the CLTCL topology.

The topology and gain curves of the CLTCL converter is presented in Fig. 2. This topology is deduced from injecting a high frequency transformer into the CLCL converter. It also possesses a RZP and accordingly harvests wide voltage gain range and current protection capacity. The impedance angle is in close proximity of zero near the first resonant point, which guarantees the primary switches smaller turn-off current and limited turn-off switching loss. Besides, the two inductors are connected in series to the primary sides of the two transformers respectively, and the transformers' leakage inductors can be absorbed by the inductors, which weakens the side effects caused by parasitic parameters.

According to Fig. 1 and Fig. 2, both of the resonant tanks of LCLCL and CLTCL converters contain a pair of serial LC, and CLTCL also contains a parallel structure comprised of capacitor $C_2$, inductor $L_2$ and transformer $T_2$. In consequence, the semblable topologies make it possible to integrate the two different MRCs into one.

One possible integrated topology is shown in Fig. 3. In the primary side of the resonant network, $L_1$ and $C_1$ form the serial $LC$ pair, while $C_2$, $L_2$ and the auxiliary transformer $T_2$ constitute the parallel cell. The secondary side switches take charge to morph the equivalent topology of the converter so that it changes over between LCLCL and CLTCL. $S_{a1}$ and $S_{a2}$ can adopt the IGBT without the anti-body-diode or a pair of MOSFET arranging as illustrated in Fig. 3. Besides, to reduce the magnetic component, $L_2$ is substituted by the leakage inductor of $T_2$. The specific operation principles are analyzed in the next section.

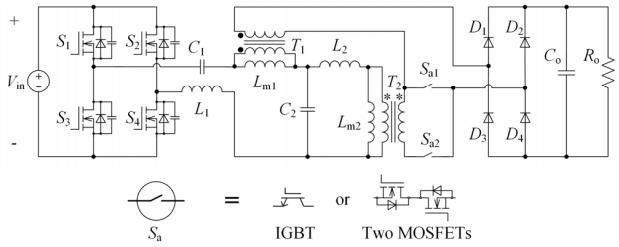


Fig. 3. The topology of the topology morphing MRC.

## III. Operation Principle

The proposed converter owns different gain curves through morphing the equivalent topologies, thus enjoying high efficiency among wide gain range. Fig. 4 presents the four equivalent topologies.

Topology 1: As shown in Fig. 4(a), $S_1$ – $S_4$ work as the full-bridge inverter. $S_{a1}$ conducts and $S_{a2}$ is off. Transformer $T_2$ is disabled. Accordingly, the magnetizing inductor $L_{m2}$ is integrated with $L_2$ as the equivalent parallel inductor $L_{eq2}$ of the LCLCL topology. At the rated situation, the converter will operate as the full-bridge LCLCL (FB-LCLCL), which is able to transfer 3rd harmonics and obtains limited circulating energy.

Topology 2: The half-bridge LCLCL (HB-LCLCL) is similar with that in Fig. 4(a) except for that $S_2$ is turned off and $S_4$ is turned on permanently. It ensures the converter step-down conversion as well as high efficiency simultaneously.

Topology 3: In Fig. 4(b), $S_{a1}$ is shut down and $S_{a2}$ is turned on. $T_2$ is enabled and the integration of $L_{m2}$ and $L_2$ is cancelled. The circuit is working under the full-bridge CLTCL (FB-CLTCL) condition, where this topology is used for high voltage gain requirement.

Topology 4: The half-bridge CLTCL (HB-CLTCL) circuit is also similar with the FB-CLTCL except for the inverter part. Since the voltage gain of the half-bridge topology is half of its full-bridge counterpart, the HB-CLTCL is applied as the transitional stage between the FB-CLTCL and the FB-LCLCL and provides middle level voltage gain.

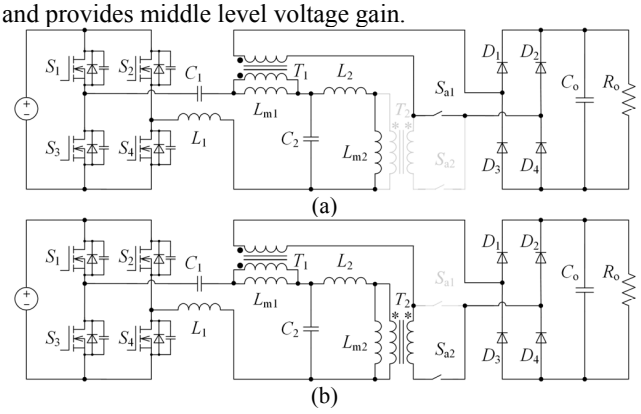


Fig. 4. Equivalent topologies of the proposed converter. (a) Full-bridge CLTCL. (b) Full-bridge LCLCL.

Related to the analyses above, the proposed converter can shift its equivalent topology for the purpose of adjusting voltage gain within a narrow frequency range. Although switches $S_{a1}$ and $S_{a2}$ introduce extra conduction losses, they are arranged at the secondary side, at which the output voltage is high and therefore the output current is low. The low output current restricts the conduction loss greatly, and the detrimental influence on the total efficiency can be ignored. Besides, with the help of $S_{a1}$ and $S_{a2}$, the converter is operated near the resonant points throughout and avoids the potential high frequency losses.

## IV. Parameter Design

The topology morphing converter is one kind of MRC, so the multiple resonant parameters must be designed for desirable conversion performance.

### A. The LCLCL Topology

For the LCLCL converter, the three resonant frequency points $f_{L01}$, $f_{L02}$ and $f_{L03}$ are calculated as equations (1) - (3) through first harmonic approximation (FHA), where $L_{eq2} = L_{m2} + L_2$.

$$f_{L01} = \frac{1}{2\pi}\sqrt{\frac{L_1C_1 + L_{eq2}C_2 + L_{eq2}C_1 - \sqrt{(L_1C_1 + L_{eq2}C_2 + L_{eq2}C_1)^2 - 4L_1L_{eq2}C_1C_2}}{2L_1L_{eq2}C_1C_2}} \tag{1}$$

$$f_{L02} = \frac{1}{2\pi}\frac{1}{\sqrt{L_{eq2}C_2}} \tag{2}$$

$$f_{L03} = \frac{1}{2\pi}\sqrt{\frac{L_1C_1 + L_{eq2}C_2 + L_{eq2}C_1 + \sqrt{(L_1C_1 + L_{eq2}C_2 + L_2C_1)^2 - 4L_1L_{eq2}C_1C_2}}{2L_1L_{eq2}C_1C_2}} \tag{3}$$

These resonant points should be arranged as (4). $f_{L01}$ here is set at 100kHz.

$$f_{L01} : f_{L02} : f_{L03} = 1 : 2 : 3 \tag{4}$$

Through (4), under the LCLCL mode, the converter will transfer the 1st and 3rd power simultaneously at rated, since the corresponding gain curves have two resonant points located at 1st and 3rd as shown in Fig. 1. Instead of ringing as the circulating power as the traditional LLC converter does, the 3rd harmonic is employed to transfer active power, and hence the circulating power is limited.

From the aspect of RZP, $f_{L02}$ locates in the middle of $f_{L01}$ and $f_{L03}$. For one thing, $f_{L02}$ should not be far away from $f_{L01}$ otherwise the voltage gain cannot be regulated within the narrow frequency scope; for another, the RZP is prevented from staying closely to resonant points, or it will cause rapid increase of the input impedance angle and bring in promoted conduction losses [15]. As a consequence, (4) is made for compromise.

### B. The CLTCL Topology

Similar with the LCLCL topology, the resonant points for CLTCL are calculated at first as (5) – (7), where $N_2$ is the turns ratio of $T_2$.

$$f_{C01} = \frac{1}{2\pi}\sqrt{\frac{\frac{1}{C_1}(\frac{L_{m1}}{N_1^2} + \frac{L_{m2}}{N_2^2})}{(L_1 + L_{m1} + L_2 + L_{m2})(\frac{L_{m1}}{N_1^2} + \frac{L_{m2}}{N_2^2}) - (\frac{L_{m1}}{N_1} + \frac{L_{m2}}{N_2})^2}} \tag{5}$$

$$f_{C02} = \frac{1}{2\pi}\sqrt{\frac{N_1 + N_2}{N_2}\cdot\frac{1}{C_2(L_2 + L_{m2})}} \tag{6}$$

$$f_{C03} = \frac{1}{2\pi}\sqrt{\frac{(L_1 + L_{m1} + L_2 + L_{m2})(\frac{L_{m1}}{N_1^2} + \frac{L_{m2}}{N_2^2}) - (\frac{L_{m1}}{N_1} + \frac{L_{m2}}{N_2})^2}{C_2[\frac{(L_2 + L_{m2})L_1L_{m1}}{N_1^2} + \frac{(L_1 + L_{m1})L_2L_{m2}}{N_2^2}]}} \tag{7}$$

Similar with the LCLCL topology, the resonant points of the CLTCL topology are also selected by placing the resonant frequency points and peak voltage gain values.

### C. The Compound Voltage Gain Curve

In this paper, the chosen parameters are listed in Table 1.

TABLE I. Resonant Parameters of the Proposed Converter

| Component | Value | Component | Value |
|---|---|---|---|
| $L_1$ | 100μH | $L_{m1}$ | 395μH |
| $L_2$ | 3μH | $N_1$ | 1.5 |
| $C_1$ | 11nF | $L_{m2}$ | 91μH |
| $C_2$ | 6.7nF | $N_2$ | 11.5 |

The compound voltage gain curve is presented in Fig. 5. It indicates that four curves constitute this compound gain curve. $M_{Cgain}(f_{C01})$ of the FB-CLTCL exceeds 8 and shows wide voltage gain range within a very small $f_s$ range from $f_{Lp}$ to $f_{L01}$. The proposed converter works at Topology 1 for high voltage gain range from 4 to 8 and at Topology 2 within $M_{Cgain}$ range of 3 to 4.

When the demand for high voltage gain is weakened, the converter transfers its topology from HB-CLTCL to FB-LCLCL. The converter reaches its rating point around $f_{L01}$, at which both of the 1st and 3rd harmonics powers are employed

to deliver active power. The circulating energy is thereby constrained. In topology 4, the HB-LCLCL topology ensures the converter step-down operation. Since the operating frequency $f_s$ is still near the rating frequency point, high efficiency is also guaranteed.

Related to the above analyses, the proposed converter possesses a broadened voltage gain range from 0.75 to 8 within a very narrow frequency range from $0.67f_{L01}$ to $f_{L01}$. The narrow $f_s$ range and 3rd power transmission contributes to high efficiencies among almost full voltage gain range, which make the topology morphing MRC competitive for high step-up applications.

Besides, the existing of $f_{L02}$ also ensure the converter inherent over-current protection without large elevation of the operating frequency.

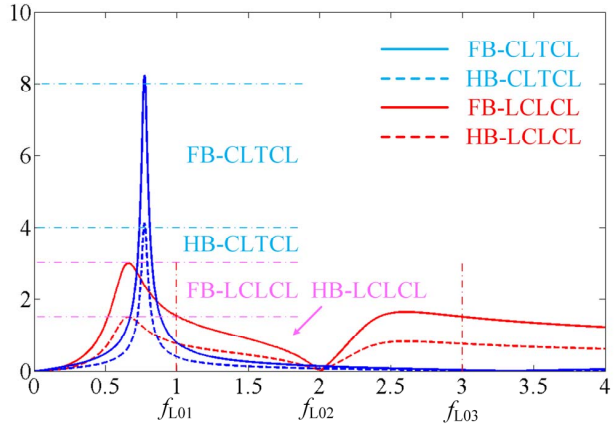


Fig. 5. The compound voltage gain curve.

## V. Exprimental Results

To verify the performance of the proposed converter, a prototype is fabricated and tested.

Fig. 6 presents the experimental waveforms of the rating condition. The converter works at the FB-LCLCL mode, where the input voltage $v_{in}$ is 133.3V, the output voltage $v_o$ is 202.2V, the operating frequency is 100kHz and the power is 200W. $v_{S1}$ and $i_{S1}$ are defined as the voltage and the current of switch $S_1$, and $i_{D1}$ represents the current through $D_1$. It is seen clearly that unlike the normal LLC converter, $i_{S1}$ contains the 1st and 3rd order harmonics simultaneously, and thereby it shows a saddle-shaped waveform. The utilization of the high order harmonic power contributes to the reduction of the circulating energy. In consequence, high efficiency of 98.1% is guaranteed at rated.

Waveforms of $v_{S1}$, $i_{S1}$, $i_{D1}$ and $v_o$ at the light load condition is shown in Fig. 7, where $v_{in}$ equals to 24.8V, $v_o$ is 200.5V and the power is 50W. The converter operates at the FB-CLTCL mode, and the corresponding voltage gain reaches as high as 8.08. Besides, it is clearly shown that the turn-off current of $S_1$ and the turn-on current of $D_1$ are both in close approximation to zero, and accordingly all the turn-on and turn-off processes of the primary-side switches and the secondary-side diodes realize soft-switching or quasi-soft-switching, which greatly restricts the switching losses of the converter.

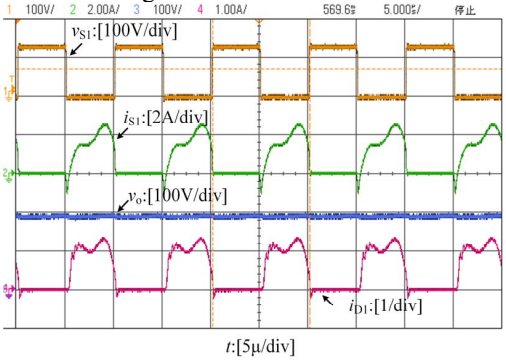


Fig. 6. Experimental waveforms at the rating condition.

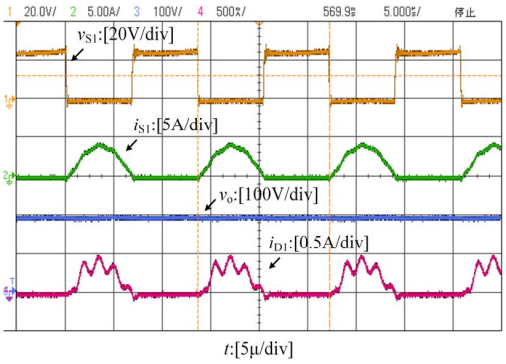


Fig. 7. Experimental waveforms at the light load condition.

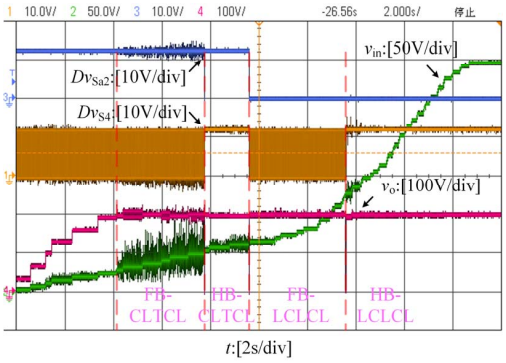


Fig. 8. Experimental waveforms of $v_{in}$ increasing from 0V to 300V.

Fig. 8 reflects the performance of the regulation for the output voltage. $Dv_{Sa2}$ and $Dv_{S4}$ are the drive signals of switch $S_4$ and auxiliary switch $S_{a2}$ respectively. It can be seen that the output voltage $v_o$ is controlled almost constant at 200V with only a 3% ripple when the input voltage $v_{in}$ varies from 25V to 300V. When $v_{in}$ reaches 25V, the converter works as the FB-CLTCL circuit to pursue high voltage gain. The auxiliary switches $S_{a2}$ is turned on constantly. This topology maintains $v_o$ stable within a narrow frequency range, when $v_{in}$ is from 25V to 50V. Then with the further increase of $v_{in}$, the proposed converter transfers its equivalent topology to the HB-CLTCL. $S_{a2}$ keeps on-state, and $S_2$, $S_4$ are turned off and on respectively. In this mode, the regulated $v_o$ is also ensured within $v_{in}$ range

from 50V to 66.7V. The converter enters into the FB-LCLCL mode if $v_{in}$ continues to increase and is larger than 66.7V. In this mode, $S_{a2}$ turns off and $S_{a1}$ conducts. The voltage gain varies from 3 to 1.5, corresponding to $v_{in}$ range of 66.7V to 133V, and $v_o$ is still maintained at 200V. The converter operates as the HB-LCLCL topology if $v_{in}$ exceeds 133V. Similar with the HB-CLTCL, $S_4$ is set on permanently in this mode. The converter changes from the step-up state to the step-down state, since $v_{in}$ rises exceeding 200V from 133V. Moreover, $v_o$ keeps constant at 200V as well when $v_{in}$ changes from 133V to 300V.

This figure demonstrates the proposed converter possesses the capability to provide widely adjustable voltage gain from less than 0.67 to 8 through topology morphing, which helps to regulate the output voltage within wide input voltage range. Besides, also being beneficial from the topology morphing feature, the operating frequency range is relatively small, and this exhibits higher efficiency potentially.

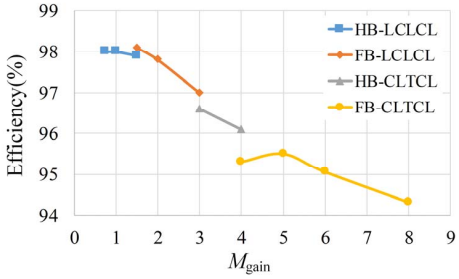


Fig. 9. Efficiency curves of different topologies.

The efficiencies of different topologies are presented in Fig. 9. Since the proposed converter works at four different topologies along with the variations of $v_{in}$, four efficiency curves, relevant to diverse voltage gain ranges, are presented. These curves are measured at 200W with various input voltages. It shows that the converter obtains relatively high efficiency within wide voltage gain range. The highest efficiency reaches 98.1%, and maintains around 98% on the condition when $v_{in}$ > 100V ($M_{gain}$ < 2). This is because with identical power levels, the converter's input current of higher $v_{in}$ is much smaller than that of lower $v_{in}$. Main losses as the conduction losses and magnetic losses are significantly related to the amplitudes of currents, and hence higher current will increase losses progressively.

## CONCLUSION

In this paper, a topology morphing MRC is proposed. The converter can operate at four different topologies, including FB-CLTCL, HB-CLTCL, FB-LCLCL and HB-LCLCL. By this way, broadened voltage gain range has been achieved within a limited operating frequency range, while maintaining relatively high efficiencies at the same time. In the end, a prototype is established to verify the performance of the proposed converter, whose highest efficiency is as high as 98.1%.

## REFERENCES


[1] C. Wang, L. Yang, Y. Wang, Z. Meng, W. Li, and F. Han, "Circuit configuration and control of a grid-tie small-scale wind generation system for expanded wind speed range," *IEEE Trans. Power Electron.*, vol. 32, no. 7, pp. 5227-5247, Jul. 2017.

[2] M. I. Shahzad, S. Iqbal, and S. Taib, "A wide output range HB-2LLC resonant converter with hybrid rectifier for PEV battery charging," *IEEE Transactions on Transportation Electrification*, vol. 3, no. 2, pp. 520-531, Jun. 2017.

[3] B. Hamed, and K. Ferid, "Double modulation control scheme for a DC/DC converter applied to a battery charger," *IET Power Electron.*, vol. 7, no. 8, pp. 2022-2029, 2014.

[4] B. R. Lin, "Modular resonant DC/DC converter for DC grid system applications," *IET Renewable Power Generation*, vol. 11, no. 7, pp. 952-958, May 2017.

[5] X. Li, and A. K. S. Bhat, "Analysis and design of high-frequency isolated dual-bridge series resonant DC/DC converter," *IEEE Trans. Power Electron.*, vol. 25, no. 4, pp. 850-862, Apr. 2010.

[6] X. Qu, S. C. Wong, and C. K. Tse, "An improved LCLC current-source-output multistring LED driver with capacitive current balancing," *IEEE Trans. Power Electron.*, vol. 30, no. 10, pp. 5783-5791, Oct. 2015.

[7] H. Wu, Y. Li, and Y. Xing, "LLC resonant converter with semiactive variable-structure rectifier (SA-VSR) for wide output votlage range application," *IEEE Trans. Power Electron.*, vol. 31, no. 5, pp. 3389-3394, May 2016.

[8] H. Wu, X. Zhan, and Y. Xing, "Interleaved LLC resonant converter with hybrid rectifier and variable-frequency plus phase-shift control for wide output voltage range applications," *IEEE Trans. Power Electron.*, vol. 32, no. 6, pp. 4246-4257, Jun. 2017.

[9] S. Hu, J. Deng, C. Mi, and M. Zhang, "Optimal design of line level control resonant converters in plug-in hybrid electric vehicle battery chargers," *IET Elect. Syst. Transp.*, vol. 4, no. 1, pp. 21-28, Mar. 2014.

[10] X. Fang, H. Hu, F. Chen, U. Somani, E. Auadisian, J. Shen, and I. Batarseh, "Efficiency-oriented optimal design of the LLC resonant converter based on peak gain placement," *IEEE Trans. Power Electron.*, vol. 28, no. 5, pp. 2285-2296, May 2013.

[11] X. Fang, H. Hu, Z. J. Shen, and I. Bataseh, "Operation mode analysis and peak gain approximation of the LLC resonant converter," *IEEE Trans. Power Electron.*, vol. 27, no. 4, pp. 1985-1995, Apr. 2012.

[12] Z. Liang, R. Guo, J. Li, and A. Q. Huang, "A high-efficiency PV module-integrated DC/DC converter for PV energy harvest in FREEDM systems," *IEEE Trans. Power Electron.*, vol. 26, no. 3, pp. 897-909, Mar. 2011.

[13] H. Hu, X. Fang, F. Chen, Z. J. Shen, and I. Bataseh, "A modified high-efficiency LLC converter with two transformers for wide input-voltage range applications," *IEEE Trans. Power Electron.*, vol. 28, no. 4, pp. 1946-1960, Apr. 2013.

[14] J. H. Jung, H. S. Kim, M. H. Ryu and J. W. Baek, "Design methodology of bidirectional CLLC resonant converter for high-frequency isolation of DC distribution systems," *IEEE Trans. Power Electron.*, vol. 28, no. 4, pp. 1741-1755, Apr. 2013.

[15] D. Fu, F. C. Lee, Y. Liu, and M. Xu, "Novel multi-element resonant converters for front-end dc/dc converters," *in Proceedings of the IEEE Power Electronics Specialists Conference*, pp. 250~256, Rhodes, Jun. 2008.

[16] C. Wang, L. Yang, Y. Wang, and B. Chen, "A 1kW CLTCL resonant DC-DC converter with restricted switching loss and broadened voltage range," *IEEE Trans. Power Electron.*, vol. pp, no. pp, pp. 1-1, 2017.